Application of Higher Order Fission Matrix for Real Variance Estimation in McCARD Monte Carlo Eigenvalue Calculation

Ho Jin Park [a*] and Hyung Jin Shim [b]
[a]*Korea Atomic Energy Research Institute , 111, Daedeok-daero 989beon-gil, Daejeon, 305-353, Korea*
[b]*Seoul National University, 1 Gwanak-ro, Gwanak-gu, Seoul 151-742, Korea*
[*]*Corresponding author: parkhj@kaeri.re.kr*

1. Introduction

In a Monte Carlo (MC) eigenvalue calculation, it is well known that the apparent variance of a local tally such as pin power differs from the real variance considerably. In the previous study [1], we have investigated the difference of the real to apparent standard deviation (SD) ratio due to tally size in MC eigenvalue calculations with the realistic problem such as BEAVRS [2] benchmark. It was noted that the apparent variance of a local MC tally such as pin-wise fission power or fuel assembly (FA)-wise fission power tends to be smaller than its real one while the apparent variance of the global MC tally such as k_{eff} is similar to the reference real one.

The MC method in eigenvalue calculations uses a power iteration method. In the power iteration method, the fission matrix (FM) and fission source density (FSD) are used as the operator and the solution. The FM is useful to estimate a variance and covariance because the FM can be calculated by a few cycle calculations even at inactive cycle. Recently, S. Carney have implemented the higher order fission matrix (HOFM) capabilities into the MCNP6 MC code in order to apply to extend the perturbation theory to second order [3]. Meanwhile, T. Endo proposed a theoretical model to predict the real to apparent SD ratio for local tally [4]. It was derived on the basis of HOFM and the autoregressive (AR) model in the MC eigenvalue calculations.

The purpose of this paper are to implement the HOFM capabilities into McCARD [5] and to investigate the real to apparent SD ratios with the aid of the HOFM and the Endo's theoretical method.

2. Method and Results

2.1 Higher Order Fission Matrix

A standard form of the Boltzmann transport equation can be rewritten as

$$S = \lambda \mathbf{H} S \tag{1}$$

where S and $\mathbf{H}$ are FSD and fission operator, respectively. S is defined by $S \equiv \lambda \mathbf{F} \phi$ while $\mathbf{H}$ is defined by $\mathbf{H} \equiv \mathbf{F}\mathbf{T}^{-1}$. $\mathbf{T}$ and $\mathbf{F}$ denote net loss and fission production operator in the standard form of the Boltzmann transport equation. S can be expressed as follow:

$$\begin{aligned} S^{(c)}(\vec{r}) &= \int_0^\infty \nu\Sigma_f(\vec{r},E)\phi^{(c)}(\vec{r},E)dE \\ &= \sum_{n=0}^{N} a_n^{(c)} S_n(\vec{r}), \\ S_n(\vec{r}) &\equiv \int_0^\infty \nu\Sigma_f(\vec{r},E)\phi_n(\vec{r},E)dE \end{aligned} \tag{2}$$

where $S^{(c)}(\vec{r})$ is FSD at *c*-th cycle and $\phi^{(c)}(\vec{r},E)$ is flux at *c*-th cycle. $\phi_n(\vec{r},E)$ and $S_n(\vec{r})$ is flux and FSD of n-th mode, respectively. $a_n^{(c)}$ means an expansion coefficient of n-th mode with FSD at *c*-th cycle. The coefficient can be calculated by

$$a_n^{(c)} = \frac{\left\langle S(\vec{r}) S_n^T(\vec{r}) \right\rangle}{\left\langle S_n(\vec{r}) S_n^T(\vec{r}) \right\rangle}. \tag{3}$$

In MC method, the $S_n(\vec{r})$ can be calculated by Hotelling deflation method [3]. The deflated fission matrix for n-th mode is

$$\mathbf{H}_n = \mathbf{H} - \sum_{n'=0}^{n-1} \frac{1}{\lambda_{n'}} \cdot \frac{S_{n'} S_{n'}^T}{\left\langle S_{n'} S_{n'}^T \right\rangle}. \tag{4}$$

The capabilities for the HOFM calculations are implemented into McCARD.

2.2 Verification of HOFM capability

To examine the newly implemented HOFM routines, an one-group slab homogeneous problem surrounded by a thin reflector was tested. This simple slab problem was token from the Larsen's paper [6]. The length of the central fissile region is 200 cm while the length of the left and right reflector region is only 5 cm. The central fissile regions were divided equally

into 50 mesh regions for tally. Table I presents the cross section data of the Larsen's slab problem. The MC eigenvalue calculations were performed on 2,500 total cycles with 1,000,000 neutron histories per a cycle and 1,500 inactive cycles. Table II compares the *k*-eigenvalue calculated by McCARD and MATLAB scripts. The SD of n-th mode *k*-eigenvalue, k_n, was estimated from 25 replicas with different random number sequence. The agreement between the McCARD and MATLAB seems excellent for each mode. From the results, the dominance ratio (k_1/k_0) is about 0.998.

Table I: Cross section in Larsen's slab problem [5]

Region	Location (cm)	Σ_t	$\Sigma_{s,0}$	$\nu\Sigma_f$
I	0<x<5	1.0	0.856	0
II	5<x<205	1.0	0.856	0.144
III	205<x<210	1.0	0.856	0

Table II: *k*-eigenvalue (mode 0~9)

Mode #	MATLAB	McCARD	
		k_n	$\sigma(k_n)/k_n$ (%)
0	0.999438	0.999438	0.003
1	0.997250	0.997250	0.004
2	0.993416	0.993416	0.004
3	0.987999	0.987999	0.004
4	0.981009	0.981009	0.004
5	0.972567	0.972567	0.004
6	0.962663	0.962663	0.004
7	0.951415	0.951415	0.004
8	0.938867	0.938867	0.004
9	0.925179	0.925178	0.004

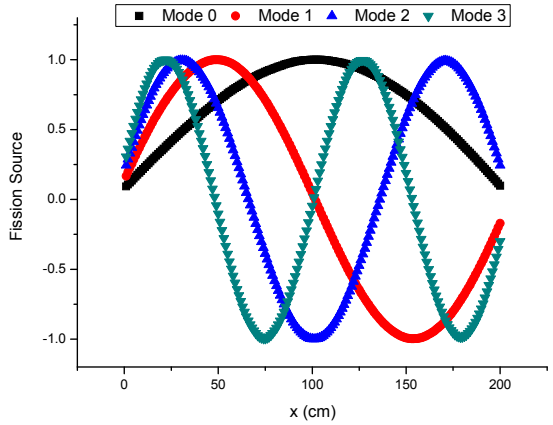

Fig. 1. Higher-order mode eigenfunction of Larsen's slab problem (mode 0 ~ 3)

Figure 1 shows the fission source eigenfunction in the range from 0-th to 3-rd mode. Figure 2 shows the cycle-wise expansion coefficients as given in Eq.(3). In the figure, the expansion coefficients from 0-th mode to 9-th mode are plotted. The fundamental mode is dominant in all the expansion coefficients. It is noted that the expansion coefficients for HOFM are slowly converged because of the inter-cycle correlation.

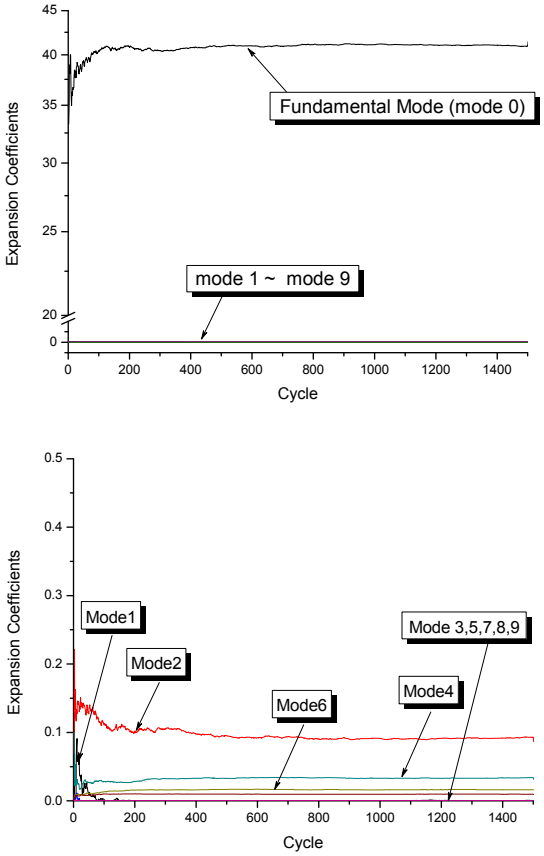

Fig. 2. Expansion coefficients of Larsen's slab problem (mode 0 ~ 9)

2.3 Behavior of Real and Apparent SD due to Mesh Size

Figure 3 and 4 compare the real and apparent SD of cell-wise fission power in 200 mesh and 20 mesh for the Larsen's slab problem. As expected, the distribution of the apparent SD in Fig. 3 and 4 appears to trying to converge to correct cosine shape, whereas the real SD has a bimodal symmetric distribution with 2 peak points, which are located at about 50 cm and 150 cm.

It can be noted first that the real SD of cell-wise fission power in 200 mesh are indeed comparable to those in 20 mesh in level and shape. However, the real to apparent SD ratio ($\sigma_{REAL}/\sigma_{APP}$) in 200 mesh differs from those in 20 mesh considerably as shown in Fig. 5. This indicated that the difference of the real to apparent SD ratio comes from the difference of the apparent SD.

The apparent SD became small as the size of the MC tally mesh increases because the increase in volume leads to the increase of track events.

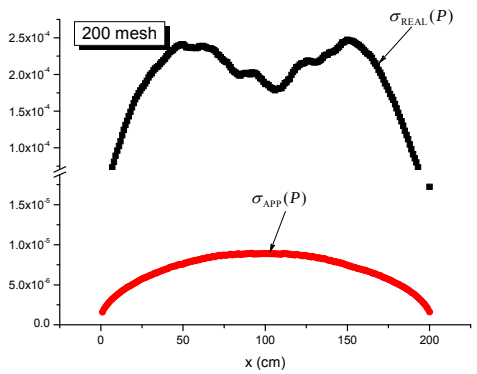

Fig. 3. Real and apparent SD of cell-wise fission power (200 mesh)

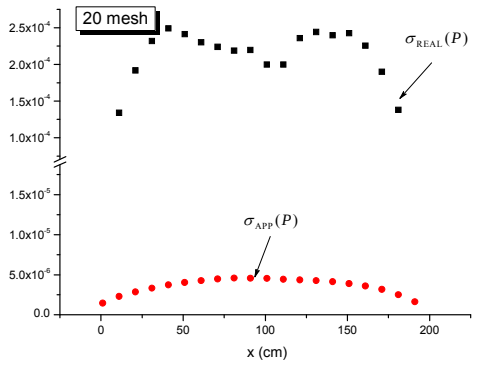

Fig. 4. Real and apparent SD of cell-wise fission power (20 mesh)

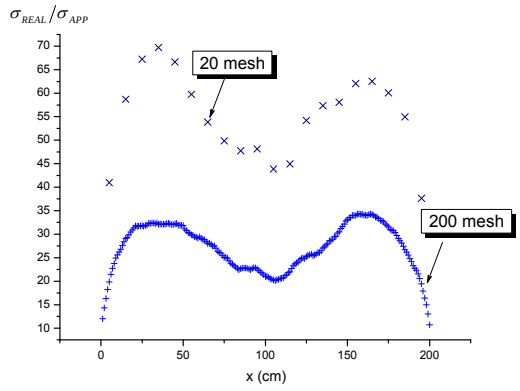

Fig. 5. Real to Apparent SD ratio of cell-wise fission power

2.4 Comparison with theoretical results by AR model

As mentioned in the introduction, T. Endo derived the theoretical formulation on the basis of higher-mode fission source distribution and the AR model. By the Endo's formulation [3], the real to apparent SD ratio can be expressed

$$\sigma_{REAL}/\sigma_{APP} \approx \sqrt{\frac{\sum_{n=1}^{\infty}\left(\frac{w_n^2}{1-\rho_n^2}\right)\cdot\left(\frac{1+\rho_n}{1-\rho_n}\right)}{\sum_{n=1}^{\infty}\left(\frac{w_n^2}{1-\rho_n^2}\right)}} \qquad (5)$$

where $w_n = \int_{V_m} S_n(\vec{r})dV$ and $\rho_n = k_n/k_0$

In this section, the real to apparent SD ratios of cell-wise fission power for one dimensional slab problems are calculated to evaluate the Endo's theoretical model. Table III shows the detailed description for two slab problem. The width of the slab is 10 cm.

Table III: Cross Section in Endo's slab problem [3]

Problem	B.C.* for both side	Σ_t	$\Sigma_{s,0}$	$\nu\Sigma_f$
I	Reflective	1.0	0.6	0.48
II	Vacuum	1.0	0.6	0.48

* B.C. = Boundary Condition

In the Endo's slab problem I, the ρ_n and $S_n(\vec{r})$ can be analytically solved

$$\rho_n \equiv \frac{k_n}{k_0} = \frac{\Sigma_a}{(1/3\Sigma_t)(n\pi/A)^2 + \Sigma_a}, \qquad (6)$$

$$S_n(x) = \begin{cases} \sin\left(\frac{n\pi}{A}x\right), & (n=1,3,5,\cdots) \\ \cos\left(\frac{n\pi}{A}x\right), & (n=2,4,6,\cdots) \end{cases} \qquad (7)$$

where Σ_t and Σ_a is the macroscopic total cross section and absorption cross section, respectively. A is the width of the slab. In the same manner, the analytic solution for the Endo's slab problem II can be calculated.

Figure 6 and 7 indicate the real to apparent SD ratios of cell-wise fission power by Endo's theoretical models. To obtain the reference solutions, the MC eigenvalue calculations were performed on 1,100 total cycles with 1,000,000 neutron histories per a cycle and 100 inactive cycles. The number of the mesh for both case is 10. The dominance ratio for Endo's slab problem I and II is about 0.918 and 0.847, respectively.

In Fig. 6 and 7, the red dot line is the reference solutions estimated from 100 replicas with different random number sequence. The black solid line is the

results by the Endo's theoretical model with the analytical solution given in Eq. (7), whereas the blue dash line is by the Endo's theoretical model with the McCARD higher-mode FM solution. The FSDs in the range from 0-th mode to 9-th mode were used for each case. It is observed that the behavior of real to apparent SD ratio in the cell-wise fission power is affected by the uncertainty of the higher-mode fission source. Overall, the Endo's theoretical model with the McCARD higher-mode FM solutions is indeed much closer to the reference than the Endo's theoretical model with the analytical solution. The difference between the Endo's models comes from the difference of the higher-mode solution between diffusion and transport theories.

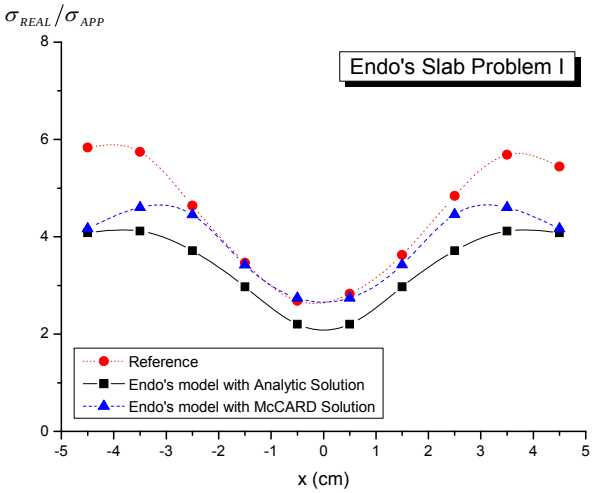

Fig. 6. Real to Apparent SD ratio of cell-wise fission power (Endo's Problem I)

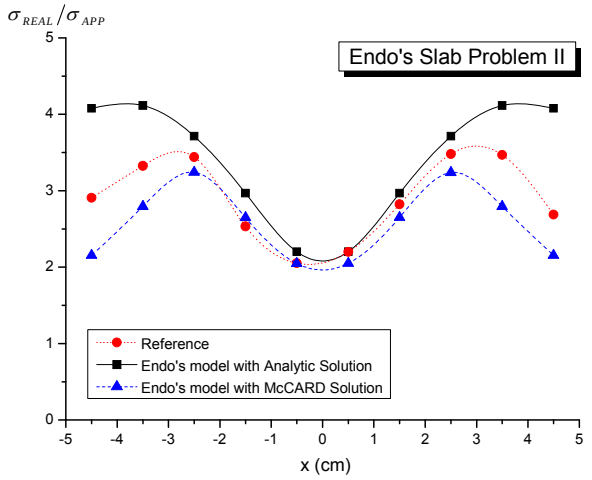

Fig. 7. Real to Apparent SD ratio of cell-wise fission power (Endo's Problem II)

3. Conclusions

In this study, the HOFM capability by the Hotelling deflation method was implemented into McCARD and used to predict the behavior of a real and apparent SD ratio. In order to predict the real to apparent SD ratio, the application of the Endo's theoretical model based on the AR model was conducted. In the simple 1D slab problems, the Endo's theoretical model predicts well the real to apparent SD ratio. It was noted that the Endo's theoretical model with the McCARD higher-mode FS solutions by the HOFM yields much better the real to apparent SD ratio than that with the analytic solutions. In the near future, the application for a high dominance ratio problem such as BEAVRS benchmark will be conducted.

REFERENCES

[1] H. J. Park, H. C. Lee, H. J. Shim, C. H. Kim, Real Variance Estimation of BEAVRS Whole Core Benchmark in Monte Carlo Eigenvalue Calculation, *Transactions of the Korean Nuclear Society Autumn Meeting*, Pyeongchang, Korea, October 30-31, 2014.
[2] N. Horelik, B. Herman, B. Forget, and K. Smith, Benchmark for Evaluation and Validation of Reactor Simulation (BEAVRS), Proc. M&C 2013, Sun Valley, Idaho, May 5-9, 2013.
[3] S. E. Carney, F. B. Brown, B. C. Kiedrowski, W. R. Martin, Higher-Mode Applcations of Fission Matrix Capability for MCNP, LA-UR-13-27078, Los Alamos National Laboratory, 2013.
[4] T. Endo, A. Yamamoto, K. Sakata, Theoretical Prediction on Underestimation of Statistical Uncertainty for Fission Rate Tally in Monte Carlo Calculation, *PHYSOR2014 – the Role of Reactor Physics Toward a Sustainable Future*, the Westin Miyako, Kyoyo, Japan, September 28 – October 3, 2014.
[5] H. J. Shim, B. S. Han, J. S. Jung, H. J. Park, C. H. Kim, McCARD: Montel Carlo Code for Advanced Reactor Design and Analysis, *Nucl. Eng. Tech.*, **44**, pp161-175, 2012.
[6] E. W. Larsen, J. Yang, A Functional Monte Carlo Method for k-Eigenvalue Problem, *Nuc .Sci. Eng.*, **159**, pp107-126, 2008.